Lithium-ion Battery State of Health Estimation Using Empirical Mode Decomposition Sample Entropy and Support Vector Machine

Sui, Xin; He, Shan; Stroe, Daniel-Ioan; Teodorescu, Remus

Published in:
2020 IEEE Applied Power Electronics Conference and Exposition (APEC)

DOI (link to publication from Publisher):
10.1109/APEC39645.2020.9124327

Publication date:
2020

Document Version
Accepted author manuscript, peer reviewed version

Citation for published version (APA):
Sui, X., He, S., Stroe, D.-I., & Teodorescu, R. (2020). Lithium-ion Battery State of Health Estimation Using Empirical Mode Decomposition Sample Entropy and Support Vector Machine. In *2020 IEEE Applied Power Electronics Conference and Exposition (APEC)* (pp. 3424-3429). Article 9124327 IEEE Press. https://doi.org/10.1109/APEC39645.2020.9124327

Lithium-ion Battery State of Health Estimation Using Empirical Mode Decomposition Sample Entropy and Support Vector Machine

Xin Sui, *Student Member*, *IEEE*, Shan He, *Student Member*, *IEEE*,
Daniel-Ioan Stroe, *Member*, *IEEE*, and Remus Teodorescu, *Fellow*, *IEEE*
Department of Energy Technology, Aalborg University
Aalborg 9220, Denmark
xin@et.aau.dk, she@et.aau.dk, dis@et.aau.dk, ret@et.aau.dk

***Abstract*—Accurate knowledge of the state of health (SOH) is important for battery management system to maintain safe operation of batteries and extend their lifetime. In order to improve the accuracy in estimating the SOH of a battery, a new method based on empirical mode decomposition sample entropy (EMDSE) and support vector machine (SVM) is proposed in this paper. Compared with the tradition SE-based method, EMD is used to filter the noise of the original signal. Then the EMDSE as a new feature is used for the SVM training, and the potential relationship between the SOH and the EMDSE is established. Finally, the effectiveness of the proposed method is verified by experimental results.**

Keywords—Lithium-ion battery, State of health, Sample entropy, Empirical mode decomposition denoising.

I. INTRODUCTION

Lithium-ion batteries have been widely applied in grid-connected energy storage systems [1], [2]. The biggest concern about the Lithium-ion batteries is their limited lifetime, as their performance deteriorates with usage. In order to guarantee the safe operation and extend the lifetime of the battery, accurate estimation of its state of health (SOH) becomes essential [3]-[5]. Generally, SOH is represented by capacity and it is defined as the ratio of the current maximum available capacity C_{now} to the initial maximum available capacity C_{ini} [6]

$$SOH = \frac{C_{now}}{C_{ini}} \times 100\% \tag{1}$$

Battery is considered to reach its end-of-life when the capacity fades by 20% of the initial value, i.e, SOH value equals to 0.8 [7]. A variety of SOH estimation methods have been proposed such as direct measurement approach and adaptive observers [8]. However, it is not feasible to test the battery capacity directly in real application, and observer-based methods not only depend on an accurate battery model but bring the computational burden for the BMS [9]. Many data-driven methods have been proposed for SOH estimation, such as neural network [10], support vector machine (SVM) [11], relevance vector machine (RVM) [12]. In these methods, the historical data of the battery are utilized for exacting features which are important to characterize the SOH of battery. Because incremental capacity peaks, the similarity of the voltage profiles or the knee points of voltage response to pulse test contain plentiful information of battery aging, they are used as features for SOH estimation [9]. Sample entropy (SE) is a powerful tool for quantitatively analyzing the complexity and predictability of signal, which is able to capture the variation of voltage, current, and temperature characteristic curves. Therefore, SE can reflect the battery aging process, and it can be used as a feature to estimate the battery SOH. In [13], SE of voltage in the full discharging process was combined with a particle filter method to estimate the battery capacity. In their later work [14], the SE of the charging temperature, charging capacity, and rest time were considered simultaneously, and the relationship between multi-variable factors and discharge capacity was established. Also using SE of the voltage in the full discharging process as the feature, the potential relationship between feature and SOH is trained by the machine learning algorithm of SVM and RVM [15]. In [16] and [17], full charging and full discharging test are replaced by the hybrid pulse power characterization test, because it takes only a few seconds and it is more efficient for feature selection. Then polynomial fitting method [16] and sparse Bayesian predictive modeling [17] were proposed, and the relationship between the SE of the voltage and the capacity can be established, so that SOH can be obtained by a battery voltage signal. However, the existing SE-based SOH estimation methods focus on the original voltage or current signals, and the effect of the measurement noise is ignored.

The collected battery data used for SOH estimation are often subject to the different levels of noise pollution due to the inner disturbances (i.e. unknown electrochemical behavior in batteries) and the impact of environmental conditions (i.e. measurement error and stochastic load) [12]. In order to further improve the estimation accuracy, data preprocessing technique is required to remove the noise of data [18]. In [12], a wavelet decomposition approach with different thresholds was introduced into the RVM model to reduce the uncertainty and improve the SOH estimation accuracy. However, in wavelet-based decomposition and reconstruction process, a suitable mother wavelet need to be set and the decomposing parameters (i.e. the number of decomposition level and the thresholds) needs to be selected manually. Unlike wavelet decomposition, the EMD technology starts from the data itself to decompose the signals, so it can separate the signals from the noise adaptive and automatic [19], [20]. In [21], an empirical mode decomposition (EMD) method was presented to generate the noise-free capacity data, and the capacity prediction is achieved by a multiple kernel RVM method. Therefore, in this paper, the original voltage signal from a battery discharging test is decomposed by the EMD method for the purpose of removing the noises, and the SE of the decomposed signal is computed as a feature to train the estimation model. Due to the advantages of solving nonlinear

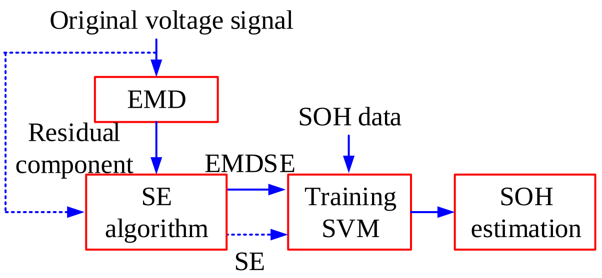

Fig.1. Schematic diagram of the proposed algorithm.

and high dimensional problems, SVM is selected to acquire the coefficient of the model. The flowchart of the proposed algorithm is illustrated in Fig. 1. Finally, aging experiments on two Lithium-ion batteries are implemented to validate the proposed method.

The rest of this paper is organized as follows. In section II, the EMD strategy and SVM modeling method are introduced. Section III presents the experiments including aging test and capacity test on two $LiFePO_4/C$ batteries. The obtained data are used for features calculation and SVM training, then the validation results are given in Section IV. Section V concludes this paper.

II. Methodology

A. Data Preprocessing Using EMD

On the basis of the concept of instantaneous frequency, N.E. Huang et al. proposed the EMD method which is used to decompose a time series into the sum of a finite number of intrinsic mode function (IMF) [20]. An IMF is a function that satisfies two the following conditions:

i) In the whole data set, the number of extrema and the number of zero crossings must either equal or differ at most by one.

ii) At any point, the mean value of the envelope defined by the local maxima and the envelope defined by the local minima is zero.

The EMD method is summarized as follows:

Step 1: For an original signal $v(t)$, all its extrema are identified;

Step 2: The upper and lower envelopes $e_{max}(t)$ and $e_{min}(t)$ can be found by cubic spline interpolating;

Step 3: The average curve $h(t)$ between the two envelopes is calculated as

$$h_1(t) = \frac{1}{2}\left(e_{max}(t) + e_{max}(t)\right) \tag{2}$$

Step 4: The remainder signal is extracted by (3)

$$c_1(t) = v(t) - h_1(t) \tag{3}$$

Step 5: Considering $c_1(t)$ as the new original signal, $h(t)$ and $c(t)$ are iteratively computed, and the result is

$$\begin{cases} h_2(t) = h_1(t) - c_2(t) \\ \quad\vdots \\ h_{nn}(t) = h_{nn-1}(t) - c_{nn}(t) \end{cases} \tag{4}$$

where nn is the number of iterations. The iterative process can be stopped by any of the following predetermined criteria, one is when the component, c_{nn}, or the residue, h_{nn}, becomes so small that it is less than the predetermined value of substantial consequence, the other is when the residue, h_{nn}, becomes a monotonic function from which no more IMF can be extracted.

During the process, $h(t)$ is regarded as the first intrinsic mode function when $h(t)$ satisfies the two requirements, one is in the whole data set, the number of extrema and the number of zero crossings must either equal or differ at most by one, the other is at any point, $h(t)$ equals to zero. The same decomposition process is repeated on $c(t)$, and the residual component in the last step of the iteration is kept as $r(t)=h(t)$. Finally, the decomposed original signal can be represented as

$$v(t) = \sum_{n=1}^{N_{EMD}} IMF_n(t) + r(t) \tag{5}$$

where N_{EMD} is the total number of IMF, $IMF_n(t)$ is the nth intrinsic mode function, and $r(t)$ is the residual component of the original voltage signal, which is used for the feature calculation in this work.

B. SE and EMDSE Calculation

Since SE can quantify the regularity of a data sequence, it can serve as the feature for SOH estimation of $LiFePO_4/C$ battery. SE (m, r, N) is defined to be the negative natural logarithm of the conditional probability (CP) that a dataset of length N, having repeated itself for m points within a boundary r, will also repeat itself for m+1 points [22]. The detail steps of the SE algorithm are shown as follows:

Step 1: For a given series {$v(1)$, $v(2)$,…, $v(N)$}, the $N-m+1$ vectors $V_m(i)$ is formed as

$$\begin{aligned} &V_m(i) = \left[v(i), v(i+1), \ldots, v(i+m-1)\right] \\ &\text{for } i = 1 \text{ to } N-m+1 \end{aligned} \tag{6}$$

Step 2: The distance between vector $V_m(i)$ and $V_m(j)$ is defined as the maximum absolute difference of their scalar elements:

$$\begin{aligned} &d[V_m(i), V_m(j)] = \max\left\{\left|v(i+k) - v(j+k)\right|\right\} \\ &\text{for } i, j = 1 \text{ to } N-m+1,\ k = 0 \text{ to } m-1 \end{aligned} \tag{7}$$

Step 3: For a given tolerance value r, W^m is computed as the number of $d[V_m(i), V_m(j)] \leq r$, and W^{m+1} is obtained by replacing m with m+1.

Step 4: The conditional probability $B_i^m(r)$ and $A_i^m(r)$ are defined as:

$$B_i^m(r) = \frac{1}{N-m-1} W^m(i), \text{ for } i = 1 \text{ to } N-m \tag{8}$$

$$A_i^m(r) = \frac{1}{N-m-1} W^{m+1}(i), \text{ for } i = 1 \text{ to } N-m \tag{9}$$

Step 5: The expression of the probability of matching points is defined as:

$$B^m(r) = \frac{1}{N-m} \sum_{i=1}^{N-m} B_i^m(r) \tag{10}$$

$$A^m(r) = \frac{1}{N-m}\sum_{i=1}^{N-m} A_i^m(r) \tag{11}$$

Step 6: By fixing m and r, SE can be obtained

$$\mathrm{SE}(m,r,N) = \lim_{N\to\infty}\left[-\ln\left[\frac{A^m(r)}{B^m(r)}\right]\right] \tag{12}$$

Because the length of the data is always limited, the SE is then estimated by the statistic.

$$\mathrm{SE}(m,r,N) = -\ln\left[\frac{A^m(r)}{B^m(r)}\right] \tag{13}$$

Typically, the parameter m is suggested to be set at 2 or 3, and r is to be set between 0.1 and 0.25 times the standard deviation of the data [22]. Because these suggestions do not always demonstrate the best results for all kinds of data set, the SE algorithm is tested using a range of parameter combinations (m=2 and 3, r ranging from 0.1-0.3 times the standard deviation of the data) [23]. Then the parameter can be chosen based on the minimization of the maximum SE relative error [24]. In the strategy for optimal selection of r, the standard approximation is used and its expression is

$$\sigma_{g(CP)} \cong |g'(CP)|\sigma_{CP} \tag{14}$$

where $g(CP)=-\log(CP)$. Then the relative error of CP estimation $\sigma_{g(CP)}$ and the relative error of SE $\sigma_{g(\mathrm{SE})}$ can be obtained by substituting $g(CP)$ into (14).

$$\sigma_{g(CP)} \cong |g'(CP)|\sigma_{CP} = \frac{\sigma_{CP}}{CP} \tag{15}$$

$$\sigma_{g(\mathrm{SE})} \cong |g'(SE)|\sigma_{CP} = \frac{\sigma_{CP}}{-\log(CP)CP} \tag{16}$$

The parameter r can be selected by minimizing the quantity which is the maximum of $\sigma_{g(CP)}$ and $\sigma_{g(\mathrm{SE})}$

$$\max\left(\frac{\sigma_{CP}}{-\log(CP)CP}, \frac{\sigma_{CP}}{CP}\right) \tag{17}$$

Finally, SE and EMDSE features can be obtained by applying the SE algorithm to the original voltage signal and to the residual component, respectively.

C. SOH Estimation Based on SVM

SVM uses kernel technique to map features vectors to high-dimensional space, which is an effective method to deal with nonlinear regression problems [11]. A SVM model is established to capture the nonlinear relationship between features and SOH. The objective of SVM is to find the optimal coefficients $\mathbf{w}$ and b on the basis of the following constrained optimization problem,

$$\begin{aligned} &\min_{w,b} \quad \frac{1}{2}\mathbf{w}^T\mathbf{w} \\ &s.t. \quad \mathbf{y}_i - \mathbf{w}^T\cdot\mathbf{x} - b \le \varepsilon \\ &\qquad\ \mathbf{w}^T\cdot\mathbf{x} + b - \mathbf{y}_i \le \varepsilon \end{aligned} \tag{18}$$

where $\mathbf{x}\in\mathrm{R}^d$ is d-dimensional input features vectors, and $y_i\in\mathrm{R}$ is SOH. After solving (18), the SOH estimation function is

$$f(\mathbf{x}) = \sum_{i=1}^{n}(\alpha_i^* - \alpha_i)K(\mathbf{x}_i,\mathbf{x}) + b \tag{19}$$

where α_i^* and α_i are Lagrange multipliers, $K(\mathbf{x}_i, \mathbf{x})$ is the kernel function. Radial basis function kernels with the form of $K(\mathbf{x}_i,\mathbf{x}) = \exp\left(-\|\mathbf{x}_i - \mathbf{x}\|^2/2\gamma\right)$ is used because it has advantages in solving nonlinear relationships.

III. Battery Testing and Degradation

The parameters of the $LiFePO_4$/C battery are shown in Table I. The $LiFePO_4$/C batteries are placed in a climatic chamber set at 25°C, and a MACCOR battery test station is used to perform the experiment. As seen in Fig. 2, the whole test consists of several rounds (38 rounds for No.1 battery and 11 rounds for No.2 battery) of aging tests and capacity tests. Batteries are aged with a one-week frequency regulation mission profile, and the battery state of charge varies from 10% and 90%. One full equivalent cycle is defined as one fully charging plus one fully discharging. For the tested 2.5Ah battery, 5Ah goes through the battery after each full equivalent cycle. There are total 4560 full equivalent cycles for No.1 battery and 1320 full equivalent cycles for No.2 battery during the overall aging process [25]. During the capacity test, the batteries are first charged with a 1C-rate constant current until the voltage reach to 3.6 V. Then the voltage is held to be 3.6 V until the current equals to 0.1 A (4% of the nominal capacity) where batteries are considered fully charged. After an hour of relaxing for keeping them electrochemically stable, the current battery capacity is measured following a 1C-rate constant current discharging procedure using a sample period of one second [26]. The battery SOH curve is obtained as shown in Fig. 3. The voltage responses for the two test batteries are presented in Fig. 4. It can be seen that during the degradation process of the batteries, the voltage curves move down. The last 360 voltage points from the constant current discharge curve are selected as original voltage signals. The original voltage signal and the corresponding residual component (obtained using the EMD technique) are shown in Fig. 5(a) and Fig. 5(b). The SE feature and EMDSE feature can be calculated, respectively, using these two set of voltage data. Based on the strategy with optimal selection of m and r, the parameters of SE algorithm are listed in Table II.

TABLE I. The Datasheet of the $LiFePO_4$/C Battery

Item	Value
Nominal capacity	2.5 Ah
Nominal voltage	3.3 V
Charge voltage	3.6 V
Cut-off voltage	2.0 V
Maximum continuous charge current	10 A
Maximum continuous discharge current	50 A

TABLE II. The Parameters of SE Algorithm

Parameters	Value
m	2
r	0.048
N	360

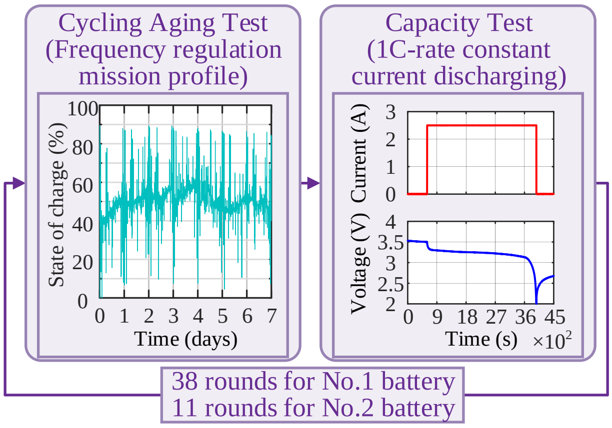

Fig.2. Flowchart of the test schedules.

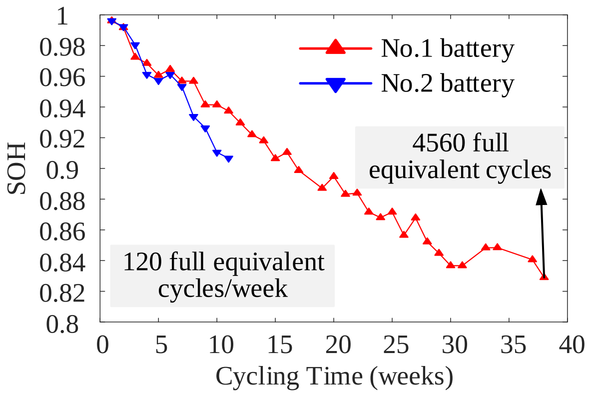

Fig.3. SOH curve of two reference batteries labeled No. 1 and No. 2.

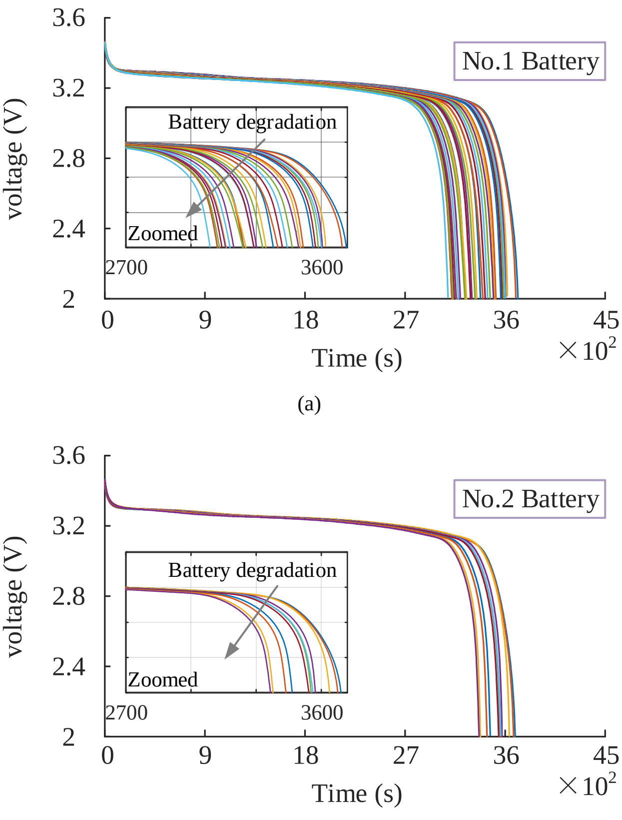

(a)

(b)

Fig.4. Voltage responses during the constant current discharging. (a) No.1 Battery; (b) No.2 Battery.

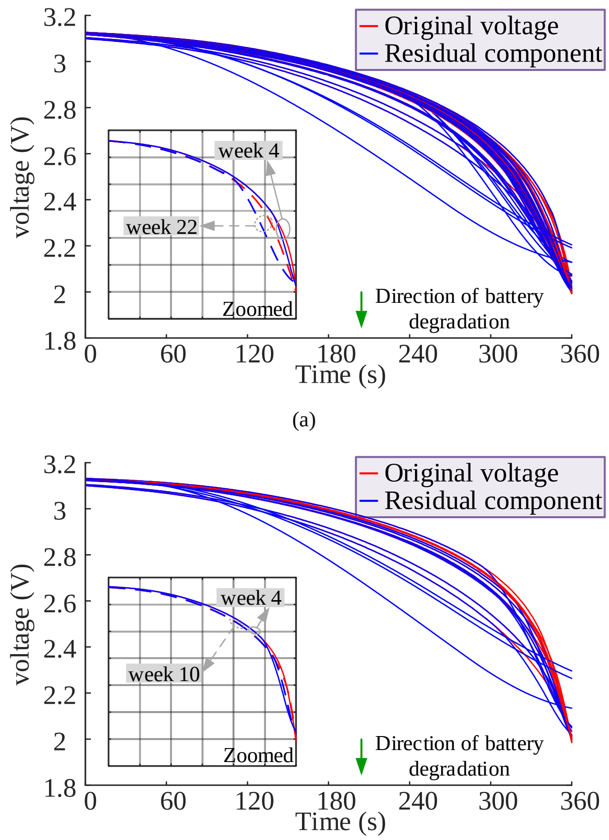

(a)

(b)

Fig.5. Original voltage signal and residual component. (a) No.1 Battery; (b) No.2 Battery.

IV. SOH Estimation

This paper uses two verification methods, which are self-validation and mutual validation, respectively. In the self-validation approach, the original voltage signal and the residual component of No.1 battery are divided into two parts. One is for SVM training, and the other is for verification. In the mutual validation approach, the original voltage signal and the residual component of No. 1 battery are used as training data, and data from No. 2 battery are used as validation data. Considering the case of mutual validation as an example, the SVM training results are shown in Fig. 6. The obtained relationship between EMDSE and SOH is more linear, which will leads a more accurate training model.

The mean percentage error (*MPE*) and the root-mean-squared percentage error (*RMSPE*) are used to evaluate the performance of the proposed method, which are defined as:

$$MPE = \frac{1}{N_T}\sum_{i=1}^{N_T} PE_i \tag{20}$$

$$RMSPE = \sqrt{\frac{1}{N_T}\sum_{i=1}^{N_T}\left(PE_i\right)^2} \tag{21}$$

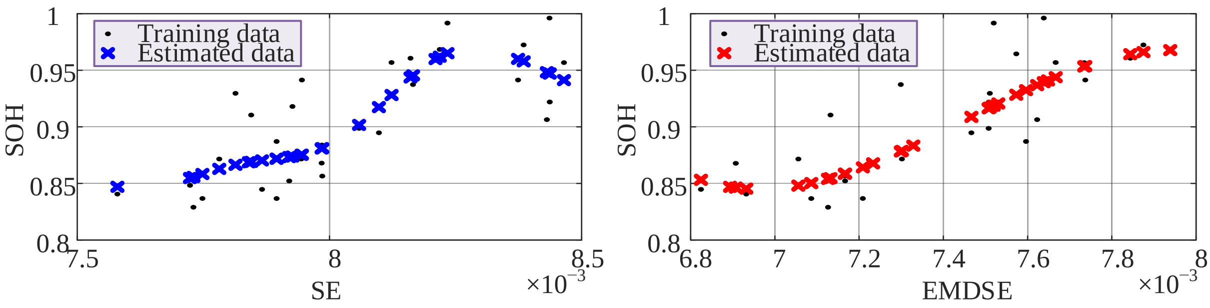

(a) (b)

Fig.6. Training results using different features. (a) SE feature; (b) EMDSE feature.

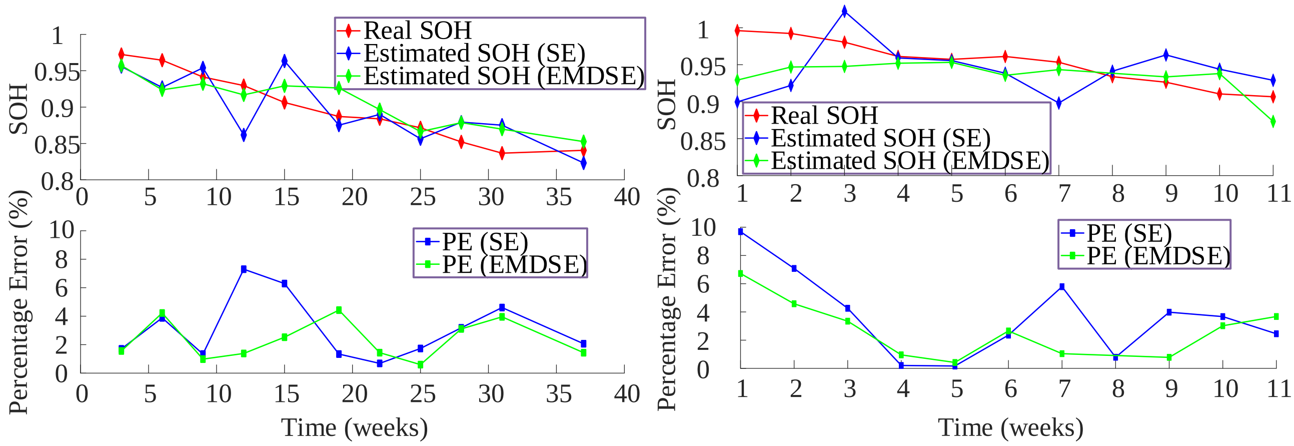

(a) (b)

Fig.7. Validation results. (a) Self-validation; (b) Mutual validation.

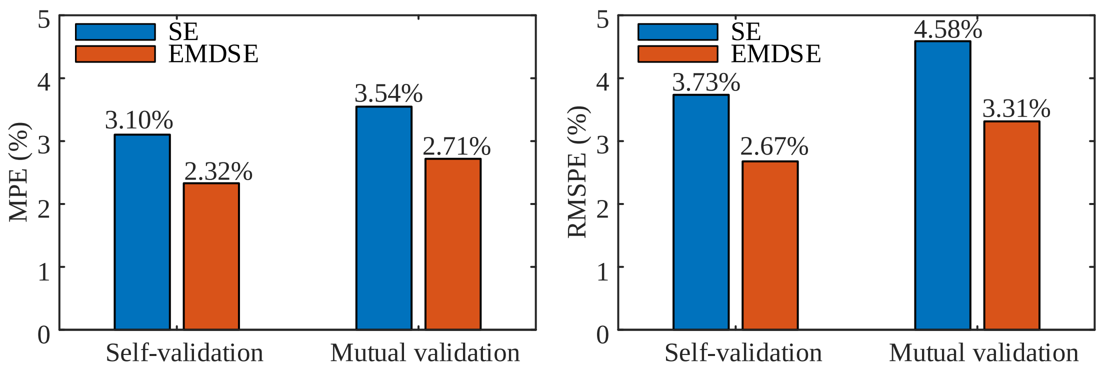

(a) (b)

Fig.8. SOH Estimation error of SVM model. (a) MPE; (b) RMSPE.

$$PE_i = \frac{\left| S\hat{O}H_i - SOH_i \right|}{SOH_i} \times 100\% \tag{22}$$

where SOH_i is the real SOH, $S\hat{O}H_i$ is the estimated SOH, PE_i is the percentage error and N_T is the total number of validation data pair. Fig. 7 shows the comparison results between the proposed algorithm (i.e., using the EMDSE as the feature) and the initial method (i.e., using the SE as the feature). Fig. 8 presents a comparison of the SOH estimation accuracy for these two algorithms. It is observed that by using EMDSE as a feature to train the SVM, the SOH estimation accuracy is improved for both self-validation and mutual validation approaches. Self-validation results show that the MPE is reduced from 3.10% to 2.32%, while the RMSPE is reduced from 3.73% to 2.67%. The accuracy of SOH estimation by mutual validation is slightly lower than that by self-validation, and the MPE of EMDSE algorithm is reduced from 3.54% to 2.71%, while the RMSPE is reduced from 4.58% to 3.31%.

V. Conclusions

This paper presents a battery SOH estimation method based on EMDSE and SVM. By applying the EMD algorithm to process an original battery voltage signal, a residual component is obtained, which is further used to generate the EMDSE. The EMDSE is used as a feature to characterize the SOH of battery. Utilizing the advantage of SVM in solving nonlinear problems, the potential relationship between the EMDSE and SOH is obtained.

Aging dada of two $LiFePO_4/C$ batteries are used for SVM model training process and validation. Experimental results show that the EMD method can reduce the noise in the original voltage signal, and the proposed algorithm based on EMDSE can improve the estimation accuracy effectively.

REFERENCES

[1] M. Świerczyński, D. I. Stroe, R. Lærke, A. I. Stan, P. C. Kjær, R. Teodorescu, S. K. Kær, "Field experience from Li-ion BESS delivering primary frequency regulation in the Danish energy market," *Ecs Trans.* vol. 61, no. 37, pp. 1-4, Sep. 2014.

[2] X. Li, D. Hui and X. Lai, "Battery energy storage station (BESS)-based smoothing control of photovoltaic (PV) and wind power generation fluctuations," *IEEE Trans. Sustain. Energy*, vol. 4, no. 2, pp. 464-473, April 2013.

[3] D. Larcher and J. M. Tarascon, "Towards greener and more sustainable batteries for electrical energy storage," *Nat. Chem.* vol. 7, no. 1, pp. 19, Jan. 2015.

[4] D. I. Stroe, V. Knap, M. Swierczynski, A. I. Stroe, and R.Teodorescu, "Operation of a grid-connected lithium-ion battery energy storage system for primary frequency regulation: A battery lifetime perspective," *IEEE Trans. Ind. Appl*. vol. 53, no. 1, pp. 430-438, Jan. 2017.

[5] D. I. Stroe, M. Swierczynski, A. I. Stan, V. Knap, R. Teodorescu, and S. J. Andreasen, "Diagnosis of lithium-ion batteries state-of-health based on electrochemical impedance spectroscopy technique," in *Proc. 2014 IEEE Energy Convers. Congr. Expo.* Pittsburgh, PA, USA, Nov. 2014, pp. 4576-4582.

[6] K.W.E. Cheng, B.P. Divakar, H. Wu, K. Ding, and H.F. Ho, "Battery-Management System (BMS) and SOC Development for Electrical Vehicles," *IEEE Trans. Veh. Technol*. vol. 60, no. 1, pp. 76-88, Jan. 2011.

[7] M. Dubarry and B. Liaw, "Identify capacity fading mechanism in a commercial $LiFePO_4$ cell," *J. Power Sources*, vol. 194, no. 1, pp. 541–549, Oct. 2009.

[8] R. Xiong, L. Li, and J. Tian, "Towards a smarter battery management system: A critical review on battery state of health monitoring methods," *J. Power Sources*, vol. 405, no. 30, pp. 18-29, Nov. 2018.

[9] Y. Li, K. Liu, A.M. Foley, A. Zülke, M. Berecibar, E. Nanini-Maury, J. Van Mierlo, and H.E. Hoster, "Data-driven health estimation and lifetime prediction of lithium-ion batteries: A review," *Renew. Sust. Energy Rev*. vol. 113, pp. 109254, Oct. 2019.

[10] H. Lin, T. Liang and S. Chen, "Estimation of battery state of health using probabilistic neural network," *IEEE Trans. Ind. Informat.* vol. 9, no. 2, pp. 679-685, May 2013.

[11] J. Meng, L. Cai, G. Luo, D. I. Stroe, and R. Teodorescu, "Lithium-ion battery state of health estimation with short-term current pulse test and support vector machine," *Microelectron. Reliab.* vol. 88, pp.1216-1220, Sep. 2018.

[12] H. Li, D. Pan and C. L. P. Chen, "Intelligent prognostics for battery health monitoring using the mean entropy and relevance vector machine," *IEEE Trans. Syst. Man, Cybern. Syst.* vol. 44, no. 7, pp. 851-862, Jul. 2014.

[13] J. Li, L. Wang, C. Lyu, W. Luo, K. Ma, and L. Zhang, "A method of remaining capacity estimation for lithium-ion battery," *Adv. Mech. Eng.* vol. 5, pp. 154831, Jan. 2015.

[14] J. Li, C. Lyu, L. Wang, L. Zhang, and C. Li, "Remaining capacity estimation of Li-ion batteries based on temperature sample entropy and particle filter," *J. Power Sources*, vol. 268, pp. 895-903, Dec. 2014.

[15] A. Widodo, M. C. Shim, W. Caesarendra, and B. S. Yang, "Intelligent prognostics for battery health monitoring based on sample entropy," *Expert Syst. Appl.* vol. 38, no. 9, pp. 11763-11769, Sep. 2011.

[16] X. Hu, S. E. Li, Z. Jia, and B. Egardt, "Enhanced sample entropy-based health management of Li-ion battery for electrified vehicles," *Energy*, vol. 64, pp. 953-960, Jan. 2014.

[17] X. Hu, J. Jiang, D. Cao, and B. Egardt, "Battery health prognosis for electric vehicles using sample entropy and sparse Bayesian predictive modeling," *IEEE Trans. Ind. Electron*. vol. 63, no. 4, pp. 2645-2656, April 2016.

[18] C. Yu, Y. Li, and M. Zhang, "Comparative study on three new hybrid models using Elman Neural Network and Empirical Mode Decomposition based technologies improved by Singular Spectrum Analysis for hour-ahead wind speed forecasting," *Energy Convers. Manage.* vol. 147, pp. 75-85, Sep. 2017.

[19] N. Chatlani and J. J. Soraghan, "EMD-based filtering (EMDF) of low-frequency noise for speech enhancement," *IEEE Trans. Audio, Speech, Language Process.* vol. 20, no. 4, pp. 1158-1166, May 2012.

[20] N.E. Huang, Z. Shen, S.R. Long, M.C. Wu, H.H. Shih, Q. Zheng, N.C Yen, C.C Tung, and H.H. Liu, "The empirical mode decomposition and the Hilbert spectrum for nonlinear and non-stationary time series analysis," *P. Roy. Soc. A-Math. Phy*. vol. 454, no. 1971, pp. 903-995, Mar. 1998

[21] C. Zhang, Y. He, L. Yuan and S. Xiang, "Capacity Prognostics of Lithium-Ion Batteries using EMD Denoising and Multiple Kernel RVM," *IEEE Access*, vol. 5, pp. 12061-12070, Jul. 2017.

[22] J. S. Richman and J. R. Moorman, "Physiological time series analysis using approximate entropy and sample entropy," *Am. J. Physiol.-Heart C.* vol. 278, no, 6, pp. H2039–H2049, Jun. 2000.

[23] J.M. Yentes, N. Hunt, K.K. Schmid, J.P. Kaipust, D. McGrath, and N. Stergiou, "The appropriate use of approximate entropy and sample entropy with short data sets," *Ann. Biomed. Eng.* Vol. 41, no. 2, pp. 349-365, Feb. 2013.

[24] D.E. Lake, J.S. Richman, M.P. Griffin, and J.R. Moorman, "Sample entropy analysis of neonatal heart rate variability," *Am. J. Physiol. Regul. Integr. Comp. Physiol.* vol. 283, no. 3, pp. R789-97, Sep. 2002.

[25] X. Sui, D.I. Stroe, S. He, X. Huang, J. Meng, and R. Teodorescu, "The effect of voltage dataset selection on the accuracy of entropy-based capacity estimation methods for lithium-ion batteries," *Appl. Sci*. vol. 9, no. 19, pp. 4170, Oct. 2019.

[26] D. I. Stroe, "Lifetime Models for lithium-ion batteries used in virtual power plants," PhD thesis, Aalborg, Denmark, Department of Energy Technology. Aalborg University, Sep. 2014.